



# *para*-Sulfonatocalix[6]arene-modified silver nanoparticles electrodeposited on glassy carbon electrode: Preparation and electrochemical sensing of methyl parathion

Yinghui Bian<sup>a</sup>, Chunya Li<sup>b</sup>, Haibing Li<sup>a,\*</sup>

<sup>a</sup> Key Laboratory of Pesticide and Chemical Biology (CCNU), Ministry of Education, College of Chemistry, Central China Normal University, Wuhan 430079, PR China

<sup>b</sup> Key Laboratory of Catalysis and Materials Science of the State Ethnic Affairs Commission & Ministry of Education, Hubei Province, South-Central University for Nationalities, Wuhan 430074, PR China

## ARTICLE INFO

### Article history:

Received 24 November 2009  
Received in revised form 20 January 2010  
Accepted 24 January 2010  
Available online 1 February 2010

### Keywords:

Electrochemical sensor  
Silver nanoparticles  
Calix[6]arene  
Methyl parathion  
Voltammetry

## ABSTRACT

In this paper, a new electrochemical sensor, based on modified silver nanoparticles, was fabricated using one-step electrodeposition approach. The *para*-sulfonatocalix[6]arene-modified silver nanoparticles coated on glassy carbon electrode (*pSC*<sub>6</sub>-Ag NPs/GCE) was characterized by attenuated total reflection IR spectroscopy (ATR-IR), X-ray photoelectron spectroscopy (XPS) and scanning electron microscopy (SEM), etc. The *pSC*<sub>6</sub> as the host are highly efficient to capture organophosphates (OPs), which dramatically facilitates the enrichment of nitroaromatic OPs onto the electrochemical sensor surface. The combination of the host–guest supramolecular structure and the excellent electrochemical catalytic activities of the *pSC*<sub>6</sub>-Ag NPs/GCE provides a fast, simple, and sensitive electrochemical method for detecting nitroaromatic OPs. In this work, methyl parathion (MP) was used as a nitroaromatic OP model for testing the proposed sensor. In comparison with Ag NPs-modified electrode, the cathodic peak current of MP was amplified significantly. Differential pulse voltammetry was used for the simultaneous determination of MP. Under optimum conditions, the current increased linearly with the increasing concentration of MP in the range of 0.01–80 μM, with a detection limit of 4.0 nM (*S/N* = 3). The fabrication reproducibility and stability of the sensor is better than that of enzyme-based electrodes. The possible underlying mechanism is discussed.

© 2010 Elsevier B.V. All rights reserved.

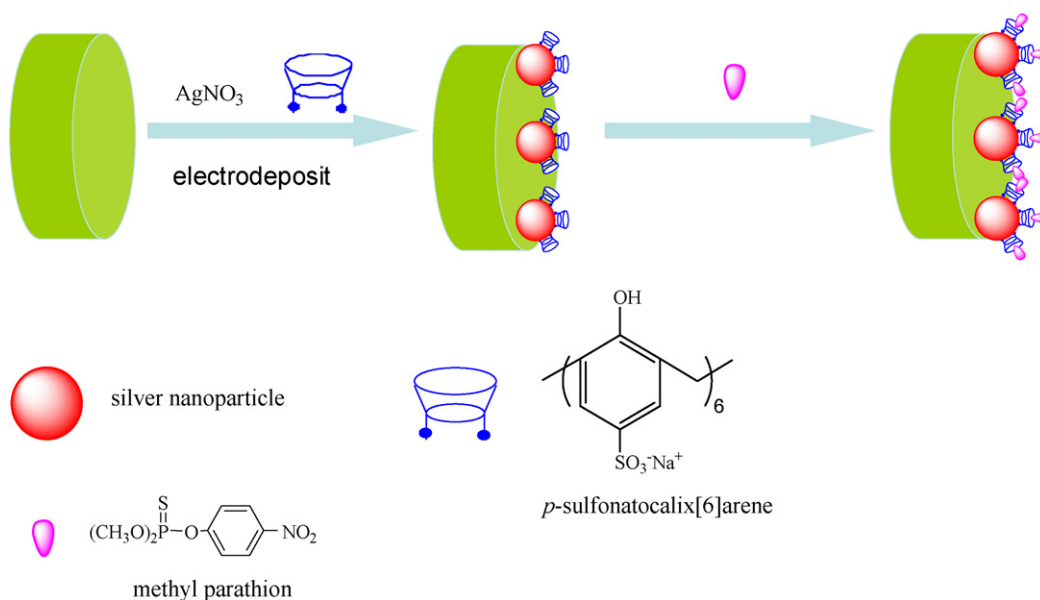
## 1. Introduction

Organophosphates (OPs) are known to be highly neurotoxic and commonly used as chemical warfare agents and pesticides [1,2]. All OPs irreversibly restrain the enzyme acetylcholinesterase (AChE), which is essential for the function of the central nervous system of humans and also of insects. The rapid detection of these toxic agents in the food, environment and public places has become increasingly important for homeland security and health protection. Analyzing OPs in environmental and food samples is routinely carried out using analytical techniques, such as gas liquid chromatography and mass spectrometry [3–7]. Although these methods are sensitive and accurate, they are generally performed at centralized laboratories, expensive instrumentation and often analysis results are not readily obtained, requiring quite some time to be available. The development of simple, cost effective, sensitive and selective analytical methods for fieldwork is of considerable interest.

Electrochemical sensors are simple, sensitive and selective devices for real-time monitoring of analytes of interest when properly designed. With the recent developments in nanotechnology, enzyme-based electrochemical biosensors towards OPs have been fabricated with nanoparticles enhancing electron transfer [8–15]. For instance, Lin and coworkers have reported a biosensor to detect OPs based on gold nanoparticles covalently coupled with acetylcholinesterase [16]. Liu's group developed a sensitive OPs sensor composed of AChE antibody linked Zn at CdS NPs and ZrO<sub>2</sub> NPs which selectively captured phosphorylated acetylcholinesterase [17]. Though these enzyme-based devices usually allow high sensitivity due to the high loading of enzymes on the nanoparticles [18–21], however, the stability of enzyme is limited since they tend to denaturation during immobilization and storage [22]. The artificial acceptors based on a host–molecule such as cyclodextrin, crown ether or calixarene, show good stability in solution and excellent binding ability towards organic molecules. *para*-Sulfonated calix[*n*]arene (*pSC*<sub>*n*</sub>) [23], a class of water-soluble calixarenes with open and rigid cavities, are interesting for molecular recognition. For instance, Barra and coworkers have showed that *pSC*<sub>*n*</sub> can recognize phenol blue by the formation of host–guest complexes [24].

\* Corresponding author. Tel.: +86 27 67866423.

E-mail addresses: [lcychem@yahoo.com](mailto:lcychem@yahoo.com) (C. Li), [lhbing@mail.ccnu.edu.cn](mailto:lhbing@mail.ccnu.edu.cn) (H. Li).



**Scheme 1.** Schematic diagram for one-step electrodeposition of *pSC*<sub>6</sub>-Ag NPs on the surface of the GCE for MP sensing.

The ability of *pSC*<sub>*n*</sub> to recognize various types of bisphenols was reported by Kitano and coworkers [25]. The *pSC*<sub>*n*</sub> is a fine stabilizer and protective agent for metallic nanoparticles [26–28]. Therefore, the fabrication of metallic NPs modified with *pSC*<sub>*n*</sub> on the surface of electrode as electrochemical sensor is quite interesting.

In this work, the fabrication of a new *pSC*<sub>6</sub> modified Ag NPs electrochemically deposited on the surface of glassy carbon electrode (GCE) is reported aiming the electrochemical detection of nitroaromatic OPs. MP was used as a model (see Scheme 1). The detection of MP was performed rapidly with detection limit (DL) of 4.0 nM (S/N = 3). The sensor opens a new opportunity for fast and sensitive determination of MP.

## 2. Experimental

### 2.1. Chemicals

Methyl parathion (MP) was provided by the Key Laboratory of Pesticide and Chemical Biology (CCNU), Ministry of Education, China. *para*-Sulfonatocalix[6]arene (*pSC*<sub>6</sub>) was synthesized in the laboratory following procedure indicated as supporting information. Phosphate buffer solution (PBS) and other reagents were of analytical reagent grade. Aqueous solutions were prepared with doubly distilled water.

### 2.2. Instruments

Electrochemical measurements were performed on CHI-660C workstation (Shanghai, China) with a conventional three-electrode system with platinum wire as auxiliary electrode, saturated calomel electrode (SCE) as reference, and *pSC*<sub>6</sub>-Ag NPs modified glass carbon electrode (*pSC*<sub>6</sub>-Ag NPs/GCE) as working electrode. Scanning electron microscopy (SEM) was recorded by a Hitachi S-4700 electron microscope. X-ray photoelectron spectroscopy (XPS) was recorded by PHI Quantera SXM. Attenuated total reflection Fourier-transform infrared spectrum (ATR-FT-IR) was acquired with a Nexus 470 FT-IR (Nicolet, USA).

### 2.3. Preparation of *pSC*<sub>6</sub>-Ag NPs modified GCE

A GCE was polished with 0.3 and 0.05 μm alumina slurry, then it was washed in a ultrasonic bath first with nitric acid solution (1:1, v/v), then with ethanol and finally with water (3 min each). The GCE was dried at room temperature.

A 0.1 M KNO<sub>3</sub> aqueous solution containing 0.2 mM AgNO<sub>3</sub> and 0.1 mM *pSC*<sub>6</sub> was used for electrodeposition of *pSC*<sub>6</sub>-Ag NPs at GCE electrodes. *pSC*<sub>6</sub>-Ag NPs were electrodeposited upon GCE electrodes by potential-sweeping electrodeposition. Electrodeposition was performed on a CHI 660 C electrochemical workstation (CH Instruments Inc.) with a conventional three-electrode system comprised of a platinum wire electrode, a SCE reference electrode, and GCE as the working electrode. The *pSC*<sub>6</sub>-Ag NPs can be formed on the GCE electrodes by cycling the potential of the working electrode between +0.40 and −0.10 V for a fixed time (for example, 110 s) [29,30]. Then the *pSC*<sub>6</sub>-Ag NPs/GCE was dipped into stirred water for 10 min to wash the excess Ag<sup>+</sup> adsorbed on the surface of the electrode. The deposited electrode was dried in air at room temperature for about 3 h. The Ag NPs/GCE was prepared under the same conditions.

### 2.4. Electrochemical measurement of MP

The PBS buffer (pH 7.4) solution, used as the supporting electrolyte and the mixed solution was purged oxygen with pure nitrogen for 10 min after addition of MP solution. The modified electrode was immersed into the electrolyte, under stirring, and the accumulation of analyte was performed during 300 s at open circuit. Differential pulse voltammograms of the modified electrode were recorded between +0.15 and −0.90 V. The cathodic peak current was measured at −0.66 V. Cyclic voltammetry was performed under similar conditions.

### 2.5. Preparation of samples

The pear commercially available was used. A HR1861, PHILIPS blender was used to comminute and homogenize the fruit samples. After filtration, the fruit juice was spiked with 5 and 60 μM of MP. For validation, fortified juice samples were analyzed after 1/100 dilution with water [3].

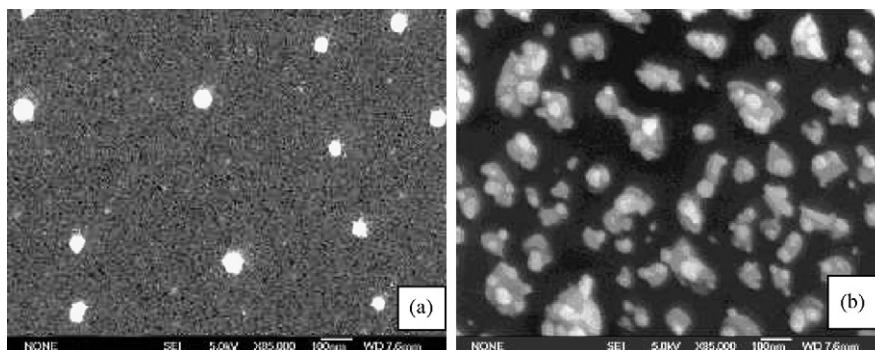


Fig. 1. SEM images of (a) Ag NPs/GCE and (b)  $pSC_6$ -Ag NPs/GCE when the electrode was magnified 85,000 $\times$ , and both the bars are 100 nm.

### 3. Results and discussion

#### 3.1. Optimization of the electrodeposition conditions and accumulation time

Three factors were considered when the electrodeposition conditions were optimized: (1) the mole ratio of  $pSC_6$  and  $Ag^+$  ( $n_{pSC_6}/n_{Ag^+}$ ), (2) the concentration of  $Ag^+$  ( $C_{Ag^+}$ ), and (3) the electrodeposition time. The cathodic peak current of MP reached the maximum when  $n_{pSC_6}/n_{Ag^+}$ ,  $C_{Ag^+}$ , and electrodeposition time were 1:2 (Fig. S1(a)),  $2 \times 10^{-4}$  M (Fig. S1(b)), and 110 s (Fig. S1(c)), respectively. Therefore, these conditions were used for further experiments.

The accumulation time for MP was studied (Fig. S2) and the maximum MP cathodic current was achieved using 300 s accumulation time. Three hundred seconds of accumulation time was thus employed in this work.

#### 3.2. Characterization of $pSC_6$ -Ag NPs/GCE electrode

The XPS survey spectrum was measured to investigate the surface of modified electrode as shown in Fig. S3. The peak at 368 and 374 eV was assigned to  $Ag^0 3d_{5/2}$  and  $Ag^0 3d_{3/2}$ , which demonstrated that metallic  $Ag^0$  was formed on the surface of GCE by electrodeposition process. Fig. 1 shows the SEM images of Ag NPs and  $pSC_6$ -Ag NPs formed on the surface of GCE by electrodeposition process, respectively. Compared with SEM image of Ag NPs on the surface of GCE (Fig. 1(a)), more  $pSC_6$ -Ag NPs were observed in Fig. 1(b). It is reasonable to believe that  $Ag^+$  ions complexed with  $pSC_6$  facilitating the reduction of  $Ag^+$  to form Ag NPs on the surface of electrode.

Fig. 2(b) and (c) shows the ATR-IR spectra of  $pSC_6$ -Ag NPs and Ag NPs electrodeposited on GCE. Compared with the FT-IR spectrum of pure  $pSC_6$  in Fig. 2(a), significant features can be seen in that of  $pSC_6$ -Ag NPs electrodeposited on GCE: the peaks for  $SO_3^-$  at 1180 and 1116  $cm^{-1}$  found in pure  $pSC_6$ , are shifted to 1166 and 1115  $cm^{-1}$ , respectively, which suggests that the  $SO_3^-$  groups coordinate with the silver atoms on the surface of the Ag NPs. The dramatic differences among the data, especially of  $SO_3^-$ , indicated that the  $pSC_6$  was modified on the surface of Ag NPs. Compared with the ATR-IR spectrum of Ag NPs on GCE (Fig. 2(c)), new peaks for  $SO_3^-$  at 1166 and 1115  $cm^{-1}$  appeared in Fig. 2(b) indicates the formation of  $pSC_6$ -Ag NPs, and the peak at 1383  $cm^{-1}$  was assigned to the  $\beta$  (O-H) of  $pSC_6$ . Similar modification with *para*-sulfonatocalix[6]arene on the surface of silver nanoparticles was shown in our previous work [26–28]. These results demonstrated that the  $pSC_6$ -Ag NPs were formed on the surface of GCE.

By using the  $Fe(CN)_6^{3-/4-}$  redox pair as the electrochemical probe, the Nyquist plots of different electrodes in the frequency ranging from 0.01 to 100,000 Hz were obtained (Fig. 3). The redox

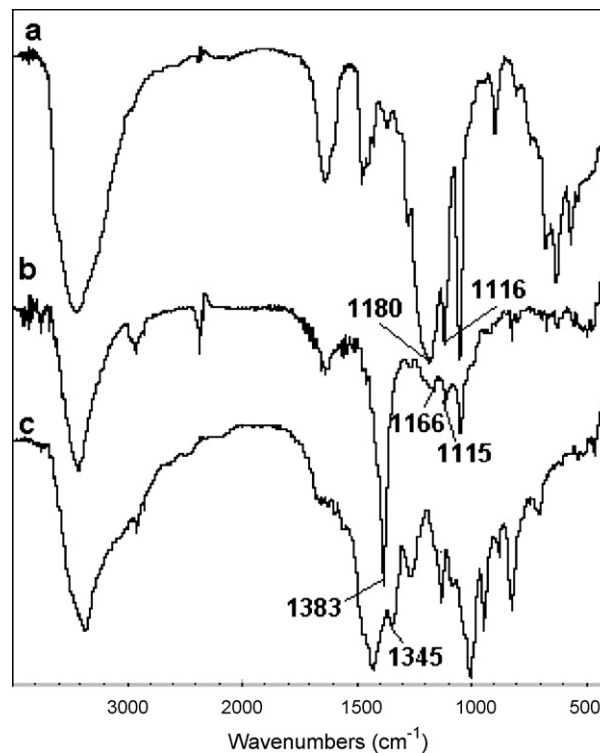


Fig. 2. FT-IR spectrum of (a)  $pSC_6$  and ATR-IR spectra of (b)  $pSC_6$ -Ag NPs and (c) Ag NPs deposited on the surface of GCE.

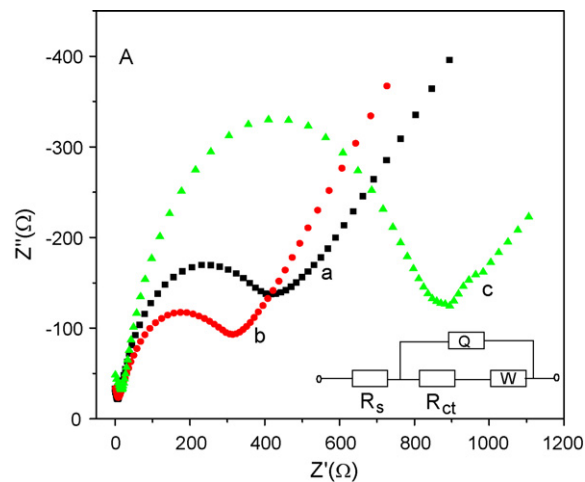
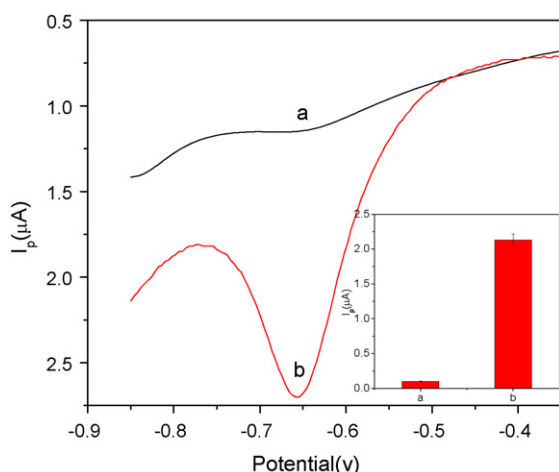


Fig. 3. (A) Electrochemical impedance spectroscopy of bare GCE (a), Ag/GCE (b) and  $pSC_6$ -Ag NPs/GCE (c) in the electrolyte containing 5.0 mM  $Fe(CN)_6^{4-/3-}$  and 0.1 M  $KNO_3$ . Inset is the equivalent circuit model used to fit the impedance data.



**Fig. 4.** Differential pulse voltammograms of  $1 \times 10^{-5}$  M MP at the Ag NPs/GCE (a); pSC<sub>6</sub>-Ag NPs/GCE (b). Inset: the current response of Ag NPs/GCE (a); pSC<sub>6</sub>-Ag NPs/GCE (b) to MP. Supporting electrolyte, 0.01 M PBS (pH 7.4); scan rate, 100 mV s<sup>-1</sup>; accumulation time, 300 s.

process of the probe showed electron transfer resistance of about 390 Ω (curve a), 310 Ω (curve b), 900 Ω (curve c) at bare GCE, Ag/GCE and pSC<sub>6</sub>-Ag NPs/GCE, respectively. It suggested that Ag NPs on the surface of GCE improved the electron transfer, and organic pSC<sub>6</sub> blocked the electron transfer which was the indirect evidence of pSC<sub>6</sub>-Ag NPs deposited on the surface of electrode.

### 3.3. The high sensitivity of electrochemical detection MP

The well-defined cathodic peaks (P1c) at -0.70 V corresponding to the irreversible reduction of -NO<sub>2</sub> to hydroxylamine group (Fig. S4, reaction 1) [29] were observed in Fig. S5. As shown in Fig. 4, the peak current (*I*<sub>p1c</sub>) of MP measured by DPV at pSC<sub>6</sub>-Ag NPs/GCE was increased significantly by 20 times compared with that obtained at the Ag NPs/GCE, which suggested that pSC<sub>6</sub>-Ag NPs/GCE displayed excellent electrochemical catalytic activities towards MP. The possible reason is as follows: hydroxylamine (-NHOH), the reduction product of MP is partly protonated in neutral media. Thus, pSC<sub>6</sub> with the electron-rich cyclic cavity and the negative SO<sub>3</sub><sup>-</sup> group can bind the aromatic and hydroxylamine of MP through host-guest interaction such as electrostatic interactions, cation-π interactions and π-π interactions [27]. And the reduction of MP may be easier in electron-rich cyclic cavity of pSC<sub>6</sub>. For these reasons, the pSC<sub>6</sub> as an artificial acceptor can bind MP via host-guest interaction and catalyze the redox of MP, simultaneously.

### 3.4. Stability of pSC<sub>6</sub>-Ag NPs/GCE

In order to test the stability of the pSC<sub>6</sub>-Ag NP/GCE, it was submitted to rigorous conditions such as strong base solution (pH 14), strong acid solution (pH 1) and boiling water (*t* = 100 °C). As shown in Fig. 5, the pretreated pSC<sub>6</sub>-Ag NPs/GCE still displayed quite good electrochemical catalytic activities towards MP, although the current intensity is decreased by about 15% and 30% for acid solution and boiling water, respectively. Generally, the enzyme would lose bioactivity under those rigorous conditions. Therefore, the stability of pSC<sub>6</sub>-Ag NPs/GCE is better than that of enzyme modified electrodes.

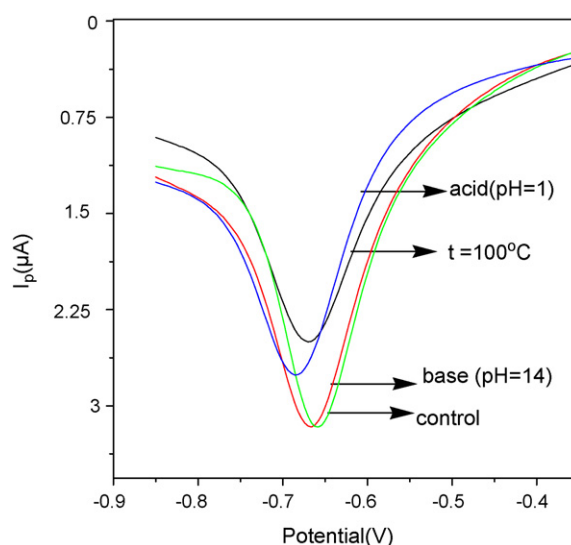
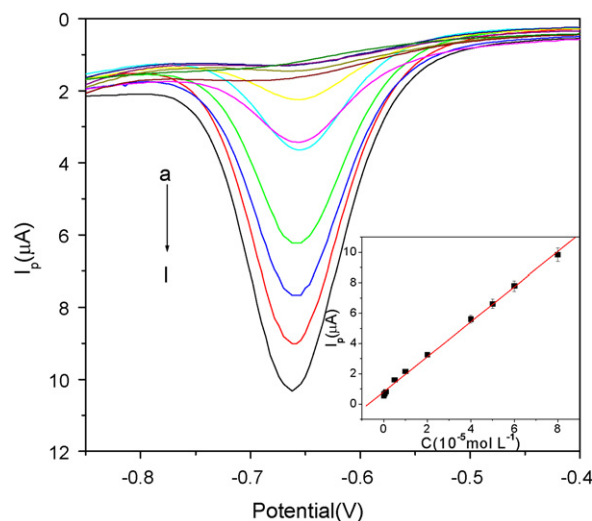


**Fig. 5.** Differential pulse voltammograms of  $1 \times 10^{-5}$  M MP at the pSC<sub>6</sub>-Ag NPs/GCE with pretreatment in strong base (pH 14), strong acid (pH 1), boiling water (*t* = 100 °C) for 10 min and without pretreatment. Supporting electrolyte, 0.01 M PBS (pH 7.4); scan rate, 100 mV s<sup>-1</sup>; accumulation time, 300 s.

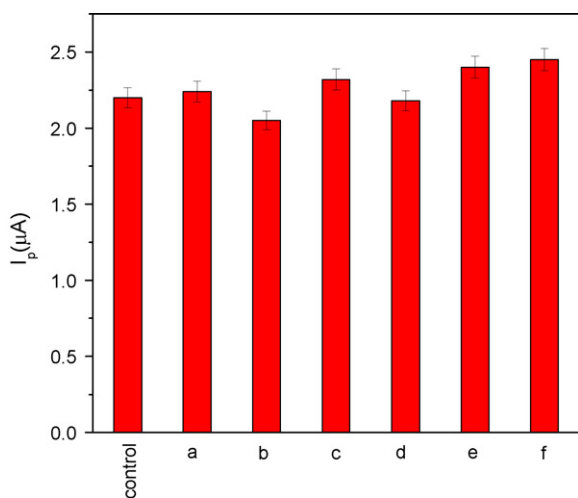
### 3.5. Analytical performance

Fig. 6 displays the DPV response of MP by pSC<sub>6</sub>-Ag NPs/GCE. The cathodic peak currents (*I*<sub>p1c</sub>) increase with the concentration of MP increasing. A linear relationship (*R*<sup>2</sup> = 0.997) between the current and the MP concentration was obtained in the range of 0.01–80 μM. The linear regression equation is *I*<sub>p</sub> (μA) = 0.76 + 1.16 × 10<sup>-5</sup> C. The detection limit (DL) of the sensor was 4 nM (*S*/*N* = 3). Though the DL of this work is higher than the DLs (0.1 nM [30], 0.4 pM [3]) of the reported OPs electrochemical sensors employing acetylcholinesterase, the stability of pSC<sub>6</sub>-Ag NPs/GCE is much better than that of enzyme modified electrodes, and the liner range is wider than some enzyme sensors (Table S1).

When the concentration of MP was controlled at 1.0 × 10<sup>-5</sup> M, good reproducibility was obtained with relative standard deviation (R.S.D.) of 4.28% for six parallel detections with the same



**Fig. 6.** Differential pulse voltammograms for MP at the pSC<sub>6</sub>-Ag NPs/GCE. MP concentration (a–l):  $1 \times 10^{-8}$ ,  $5 \times 10^{-8}$ ,  $1 \times 10^{-7}$ ,  $5 \times 10^{-7}$ ,  $1 \times 10^{-6}$ ,  $5 \times 10^{-6}$ ,  $1 \times 10^{-5}$ ,  $2 \times 10^{-5}$ ,  $4 \times 10^{-5}$ ,  $5 \times 10^{-5}$ ,  $6 \times 10^{-5}$ ,  $8 \times 10^{-5}$  M. Inset shows the calibration curve. Supporting electrolyte, 0.01 M PBS (pH 7.4); scan rate, 100 mV s<sup>-1</sup>; accumulation time, 300 s.



**Fig. 7.** The cathodic peak current response of *pSC*<sub>6</sub>-Ag NPs/GCE in solutions containing  $1 \times 10^{-5}$  M MP in the absence and presence of 100-fold of  $\text{PO}_4^{3-}$  (a),  $\text{SO}_4^{2-}$  (b),  $\text{CO}_3^{2-}$  (c),  $\text{NO}_3^-$  (d),  $1 \times 10^{-5}$  M *p*-nitrophenol (e) and nitrobenzene (f), respectively. Supporting electrolyte, 0.01 M PBS (pH 7.4); scan rate,  $100 \text{ mV s}^{-1}$ , accumulation time, 300 s.

modified electrode. Similarly, the fabrication reproducibility was estimated by using six different electrodes. A solution containing  $1.0 \times 10^{-5}$  M MP was determined by six electrodes, with a relative standard deviation of 3.6%, which indicated that the reproducibility of the electrode was excellent. The electrode retained a response of 98% of the initial current was retained for the electrode after it was stored in PBS (pH 7.4) at  $7^\circ\text{C}$  for 10 days. After a 30-day storage period, the sensor retained 95% of its initial current response, and it showed no obvious decline after being used for 30 times.

Interferences arising from the other electroactive nitrophenyl derivatives and oxygen-containing inorganic ions ( $\text{PO}_4^{3-}$ ,  $\text{SO}_4^{2-}$ ,  $\text{CO}_3^{2-}$ ,  $\text{NO}_3^-$ ) were used to evaluate the selectivity of the *pSC*<sub>6</sub>-Ag NPs/GCE to MP. Interfering experiments were performed with  $1 \times 10^{-5}$  M MP in the absence and presence of  $1 \times 10^{-5}$  M *p*-nitrophenol,  $1 \times 10^{-5}$  M nitrobenzene, 100-fold of  $\text{PO}_4^{3-}$ ,  $\text{SO}_4^{2-}$ ,  $\text{CO}_3^{2-}$  and  $\text{NO}_3^-$ . Fig. 7 shows the current signals of MP at different experimental conditions.  $\text{PO}_4^{3-}$ ,  $\text{SO}_4^{2-}$ ,  $\text{CO}_3^{2-}$ ,  $\text{NO}_3^-$  did not interfere the determination of MP with the peak current varies slightly, and *p*-nitrophenol, nitrobenzene produced scarcely any interferences though the reduction potentials of electroactive nitrophenyl derivatives are adjacent which could be partitioned. When the concentration of  $\text{PO}_4^{3-}$ ,  $\text{SO}_4^{2-}$ ,  $\text{CO}_3^{2-}$  and  $\text{NO}_3^-$  were 1000-fold of MP, these inorganic ions did not interfere the determination of MP (Fig. S7A). And as shown in Fig. S7, when the concentration of *p*-nitrophenol, nitrobenzene was 10-fold of MP, *p*-nitrophenol produced scarcely any interference, but nitrobenzene produced obviously interference, and there were obviously interferences when the concentration of *p*-nitrophenol, nitrobenzene was 10-fold of MP. These indicated that the *pSC*<sub>6</sub>-Ag NPs/GCE has potential application in the rapid determination of MP.

The concentration values of MP in the samples were determined by the proposed method. No voltammetric response corresponding to MP was observed when the real pear samples were analyzed, thus different quality of MP was added to the samples of 0.01 M PBS (pH 7.4), respectively. Standard-additions method was adopted to estimate the accuracy [31,32]. The results were summarized in Table 1. The recoveries were from 98.0% to 102.1%. These results demonstrated that it was a promising approach with high accuracy, precision and reproducibility. It can be used for the direct analysis of real relevant samples.

**Table 1**

Recovery tests of MP in pear samples ( $n=5$ ).

| Sample | Concentration taken ( $\mu\text{M}$ ) | Concentration found ( $\mu\text{M}$ ) | Recovery (%) | R.S.D. (%) |
|--------|---------------------------------------|---------------------------------------|--------------|------------|
| 1      | 5.00                                  | 5.08                                  | 101.6        | 3.2        |
| 2      | 10.00                                 | 10.21                                 | 102.1        | 4.7        |
| 3      | 20.00                                 | 19.60                                 | 98.0         | 2.2        |
| 4      | 40.00                                 | 40.50                                 | 101.3        | 4.5        |
| 5      | 50.00                                 | 51.00                                 | 102.0        | 2.6        |
| 6      | 60.00                                 | 59.50                                 | 99.2         | 3.4        |

#### 4. Conclusions

The convenient and sensitive electrochemical sensor of *pSC*<sub>6</sub>-Ag NPs/GCE opens new opportunities for the analysis of MP. The process of fabrication the modified GCE was simple and convenient, the *pSC*<sub>6</sub>-Ag NPs electrodeposited on the GCE in one-step saved much more time compared with the surface of electrode modified through self-assembled monolayer (SAM). The specific complexation of MP on the surface of homemade *pSC*<sub>6</sub>-Ag NPs/GCE showed better stability than enzyme sensor which provides an effective quantitative method for MP analysis, and in comparison with Ag NPs-modified electrode, the cathodic peak current of MP was amplified significantly. The application of the sensor for determination of MP in the samples demonstrates that it is a promising and practical approach for the analysis of MP. Further variation of the sensor system could be achieved by modifying the Ag NPs with *pSC*<sub>4</sub> or *pSC*<sub>8</sub>, thus enabling the design of sensors for other substrates.

#### Acknowledgements

This work was financially supported by the National Natural Science Foundation of China (20772038), 863 program (2009AA06A417), Program for Excellent Research Group of Hubei Province (2009CDA048), Self-determined research funds of CCNU from the colleges' basic research and operation of MOE (CCNU09AO200).

#### Appendix A. Supplementary data

Supplementary data associated with this article can be found, in the online version, at doi:10.1016/j.talanta.2010.01.054.

#### References

- [1] B.A. Du, Z.P. Li, C.H. Liu, *Angew. Chem. Int. Ed.* 45 (2006) 8022–8055.
- [2] B.A. Gorman, P.S. Francis, D.E. Dunstan, N.W. Barnett, *Chem. Commun.* (2007) 395–397.
- [3] Q. Xiao, B. Hu, C.H. Yu, L.B. Xia, Z.C. Jiang, *Talanta* 69 (2006) 848–855.
- [4] S. Lacorte, D. Barcelo, *Anal. Chem.* 68 (1996) 2464–2471.
- [5] F. Hernandez, J.V. Sancho, O.J. Pozo, *J. Anal. Bioanal. Chem.* 382 (2005) 934–946.
- [6] N. Fidalgo-Used, M. Montes-Bayon, E. Blanco-Gonzalez, A. Sanz-Medel, *Talanta* 75 (2008) 710–716.
- [7] S. Lacorte, D. Barcelo, *Environ. Sci. Technol.* 28 (1994) 1159–1163.
- [8] M.J. Banholzer, J.E. Millstone, L. Qin, C.A. Mirkin, *Chem. Soc. Rev.* 37 (2008) 885–897.
- [9] C.N. Lok, C.M. Ho, R. Chen, Q.Y. He, W.Y. Yu, H. Sun, P.K.H. Tam, J.F. Chiu, C.M. Che, *J. Biol. Inorg. Chem.* 12 (2007) 527–534.
- [10] H.D. Hill, R.A. Vega, C.A. Mirkin, *Anal. Chem.* 79 (2007) 9218–9223.
- [11] P. Zhou, Z. Dai, M. Fang, X. Huang, J. Bao, *J. Phys. Chem. C* 111 (2007) 12609–12616.
- [12] S.Q. Liu, J.H. Yu, H.X. Ju, *J. Electroanal. Chem.* 540 (2003) 61–67.
- [13] Y. Xiao, H.X. Jun, H.Y. Chen, *Anal. Chim. Acta* 391 (1999) 73–82.
- [14] X. Yu, D. Chattopadhyay, I. Geleska, F. Papadimitrakopoulos, J.F. Rusling, *Electrochem. Commun.* 5 (2003) 408–411.
- [15] E. Topoglidis, A.E.G. Cass, B. O'Regan, J.R. Durant, *J. Electroanal. Chem.* 517 (2001) 20–27.
- [16] T.J. Lin, K.T. Huang, C.Y. Liu, *Biosens. Bioelectron.* 22 (2006) 513–518.
- [17] G.D. Liu, J. Wang, R. Barry, C. Petersen, C. Timchalk, P.L. Gassman, Y.H. Lin, *Chem. Eur. J.* 14 (2008) 9951–9959.

- [18] R.E. Ionescu, C. Gondran, L.A. Gheber, S. Cosnier, R.S. Marks, *Anal. Chem.* 76 (2004) 6808–6813.
- [19] G.D. Liu, Y.H. Lin, V. Ostatna, J. Wang, *Chem. Commun.* (2005) 3481–3483.
- [20] D. Shan, S. Cosnier, C. Mousty, *Biosens. Bioelectron.* 20 (2004) 390–396.
- [21] D. Shan, M.J. Zhu, E. Han, H.G. Xue, S. Cosnier, *Biosens. Bioelectron.* 23 (2007) 648–654.
- [22] E. Shoji, M.S. Freund, *J. Am. Chem. Soc.* 123 (2001) 3383–3384.
- [23] S. Shinkai, S. Mori, T. Tsubaki, T. Sone, O. Manabe, *Tetrahedron Lett.* 25 (1984) 5315–5318.
- [24] W.L. Tao, M. Barra, *J. Org. Chem.* 66 (2001) 2158–2160.
- [25] T. Nakaji-Hirabayashi, H. Endo, H.K.M. Gemmei-Ide, H. Kitano, *Environ. Sci. Technol.* 39 (2005) 5414–5420.
- [26] D.J. Xiong, M.L. Chen, H.B. Li, *Chem. Commun.* (2008) 880–882.
- [27] D.J. Xiong, H.B. Li, *Nanotechnology* 19 (2008) 465502–465507.
- [28] C.P. Han, L.L. Zeng, H.B. Li, G.Y. Xie, *Sens. Actuators B* 137 (2009) 704–709.
- [29] M.C. Tsai, P.Y. Chen, *Talanta* 76 (2008) 533–539;  
S. Marx, A. Zaltsman, I. Turyan, D. Mandler, *Anal. Chem.* 76 (2004) 120–126.
- [30] L. Shang, Y.L. Wang, L.J. Huang, S.J. Dong, *Langmuir* 23 (2007) 7738–7744.
- [31] G. Valdés-Ramírez, D. Fournier, M.T. Ramírez-Silva, J.-L. Marty, *Talanta* 74 (2008) 741–746.
- [32] H. Schulze, E. Scherbaumb, M. Anastassiades, S. Vorlova, R.D. Schmid, T.T. Bachmann, *Biosens. Bioelectron.* 17 (2002) 1095–1105.